Electronic Supplementary Material (ESI) for Inorganic Chemistry Frontiers.

Supporting Information

An unprecedented $\{Y_2 \subset Y_{10}\}$ type disk-like Y_{12} nanocluster featuring electroluminescence property in OLED device

Lin-Ping Shi,[a] Wen-Liang Li,[a] Pu-Yue Wang,[a] Xiao-Ming Wu,[b] Zhao-Quan Yao,*[a] Jiong-Peng Zhao,*[a] and Fu-Chen Liu,*[a]*

[a] School of Chemistry and Chemical Engineering, TKL of Organic Solar Cells and Photochemical Conversion, Tianjin University of Technology, Tianjin 300384, China

[b] Key Laboratory of Display Materials and Photoelectric Devices, Ministry of Education, Tianjin Key Laboratory of Photoelectric Materials and Devices, National Demonstration Center for Experimental Function Materials Education, School of Materials Science and Engineering, Tianjin University of Technology, Tianjin 300384, China

*Corresponding authors: wxm@tjut.edu.cn; yaozq@email.tjut.edu.cn; zhaojp@tjut.edu.cn; fcliu@tjut.edu.cn.

Materials and physical characterization

All of the chemical agents and materials for synthesis were obtained commercially and used without further purification. In Y_{12}-cluster, The L^{2-} ligands were generated by the *in-situ* reaction according to the literature.[1-2] The powder X-ray diffraction (PXRD) data were characterized by using the Rigaku D/Max-2500 diffractometer with a Cu-target tube and a graphite monochromator (40 kV, 100 mA). The Simulation PXRD pattern was derived from modulating the single crystal X-ray diffraction (SCXRD) data via the Mercury (Hg) software which available free of charge via http://www. iucr.org. The FT-IR spectrum of **1** was obtained on the Bruker TENSOR 27 spectrometer and carried out by using KBr pellets dispersed with sample powders in the range from 4000 to 400 cm^{-1}. The mass spectrometry was measured by Bruker LRF and the data were collected in positive ion modes. The Ultraviolet–visible absorption spectrum was recorded on a Shimadzu UV-2600 spectrophotometer. The solid-state luminescence measurements were performed by using an Agilent Technologies Cary Eclipse photoluminescence spectrophotometer (G9800A) with a pulsed laser, which ensured the test was independent of indoor light. The lifetime and quantum yield of **1** were carried out by using the Edinburgh Instruments FLS 1000 device at room temperature. In OLED measurement, the complex film was prepared by using the hot evaporation coating machine EDWARDS BOC AUTO 500. The current density-voltage-brightness characteristics and electroluminescence (EL) spectrum of the device were measured with the computer-controlled DC power supply of a Keithley 2400 and a PR655 Spectral Photometer at room temperature. The single-crystal X-ray diffraction data of **1** at 193 K was collected with the Bruker smart Apex 2 Single Crystal X-ray Diffraction using mirror-monochromated Cu-Kα radiation (λ = 1.54178 Å) in the ω scan mode. The structure was solved by the direct method using the Olex2 1.5[3] and refined using SHELXL.[4] The non-hydrogen atoms were located in successive difference Fourier syntheses and refined with anisotropic thermal parameters on F^2. All hydrogen atoms of were generated theoretically at the specific atoms and refined isotropically with fixed thermal factors. A summary of the crystallographic data and the refinement parameters were listed in **Table S1**. The selected bond lengths and angles were listed in **Table S5 and S6**.

Synthesis of the disk-like Y_{12} cluster: $[Y_{12}(L)_{10}(CO_3)_4(NO_3)_2(\mu_3\text{-}OH)_6]$

$Y(NO_3)_3{\cdot}6H_2O$ (0.248g, 0.65mmol), 8-hydroxyquinoline (0.065g, 0.45mmol), and Na_2CO_3 (0.040g, 0.38mmol) were dissolved in 12 mL mixture solution of 8 ml C_2H_5OH and 4 ml H_2O and sealed in a 25 ml Teflon-lined stainless-steel autoclave, after that the mixture was heated at 140 °C for 3 days without disturbance. As the temperature decreased to room temperature, the light-yellow plate crystals of **1** were synthesized successfully and collected after filtration, washed with ethanol for several times, and dried in air. Yield: 43% (based on 8-hydroxyquinoline). FT-IR (cm^{-1}): 3475 (s), 3421 (s),1630 (vs), 1570 (vs), 1459 cm(vs), 1375 (vs), and 590 (m), respectively. Elemental analysis (%): calcd. for **1**: C, 52.46; H, 3.02; N, 6.60; found: C, 54.33; H, 3.32; N, 6.39.

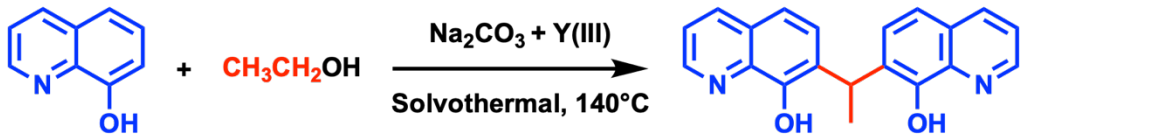

H_2L = 7,7'-(2-methylmethylene)bis(8-quinolonol)

Scheme S1. the *in-situ* reaction route of H_2L = 7,7'-(2-methylmethylene)bis(8-quinolonol).[5,6]

Preparation the complex films of and organic light-emitting device (OLED)

Before device fabrication, the complex host material (**1**) needs to be purified for twice by recrystallization. After that, the crystal sample of **1** was dissolved in DMF to obtain the precursor solution with the concentration of 5 mg/ml. For fabricating the device, the indium-tin-oxide (ITO)-coated glass was used as substate. After immersed and sonicated for 10 min in consecutively acetone, ethanol and de-ionized water, respectively. Then, the cleaned ITO-substrate was dried in the infrared drying oven and subjected to an ultraviolet-ozone for 30 min. After that, the UV-ozone-treated ITO substrate was transferred to a glove box under argon atmosphere and the hole transport layer (PEDOT:PSS) was spin coated at 3000 r/min for 30 s. After that, the 150 μl precursor solution of **1** was spin coated on the surface of PEDOT:PSS at 3000 r/min for 60 s and annealed at 100 °C for 20 min. Then, the electron transport layer (TPBi) was evaporated on the surface of **1**. Finally, the LiF/Al composite electrode was deposited on the top of the device. After fabricated, the whole device was transferred to the petri dish for testing. From bottom to top, the whole OLED device was constructed by ITO/PEDOT:PSS (40nm)/$[Y_{12}(L)_{10}(CO_3)_4(NO_3)_2(\mu_3\text{-}OH)_6]$ (110nm)/TPBi (40nm)/LiF(1nm)/Al(120nm).

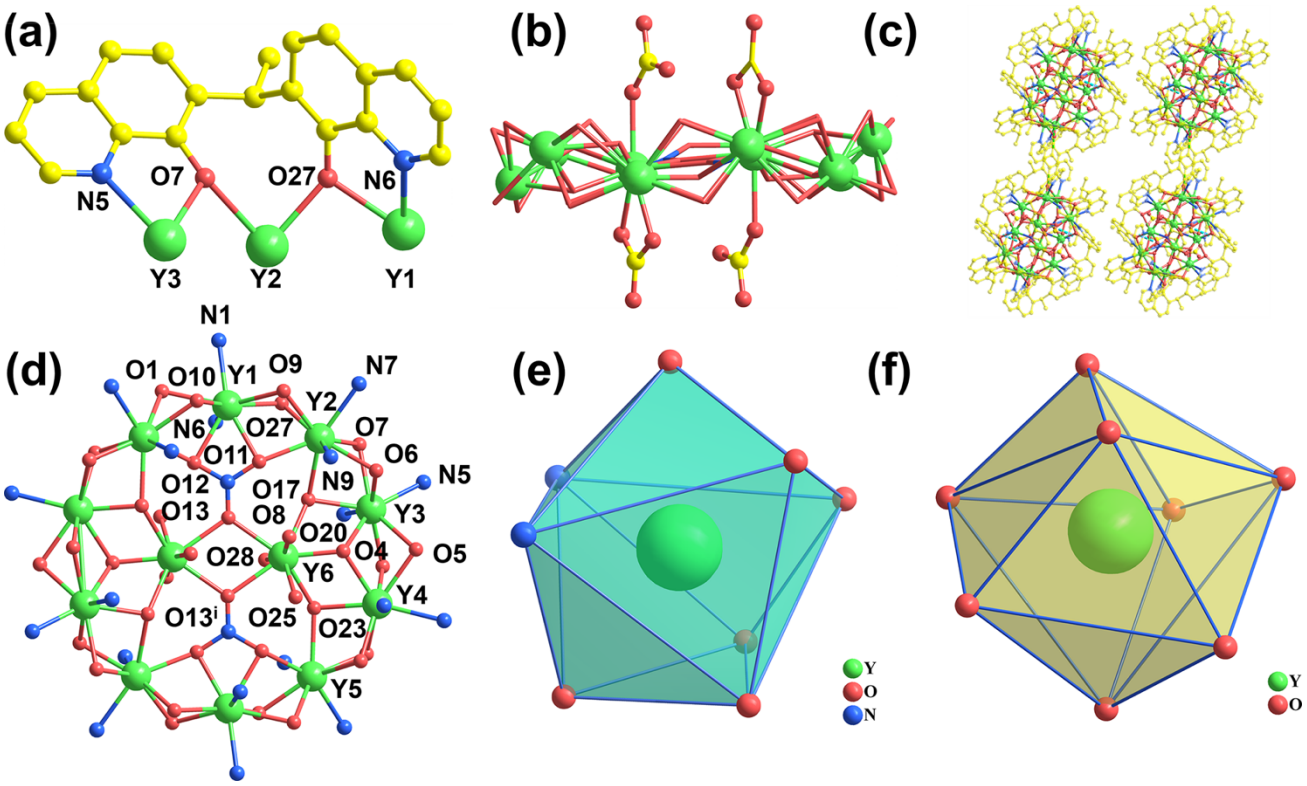

Figure S1. (a) The coordination mode of the *in-situ* organic ligand (L^{2-}) in the Y_{12} cluster. (b) The coordination pattern of the CO_3^{2-} with the Y^{3+} ions in the center of the cluster. (c) The view of the stacking mode of the Y_{12} cluster along the *b*-axis. (d) The coordination diagram of the Y-O-N core. (e) and (f) The coordination environments of the two types of the Y^{3+} ions in cluster **1**. Symmetry codes: ^{i}1-x, 1-y, 1-z.

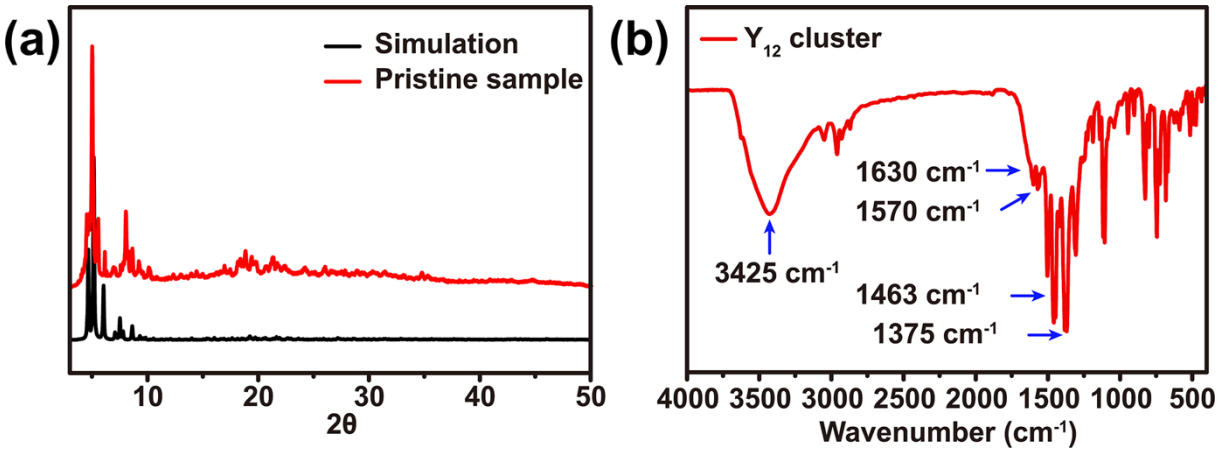

Figure S2. (a) The PXRD pattern of the Y_{12} cluster. (b) The FT-IR spectrum of the disk-like Y_{12} cluster, the main peaks have been indexed, respectively.

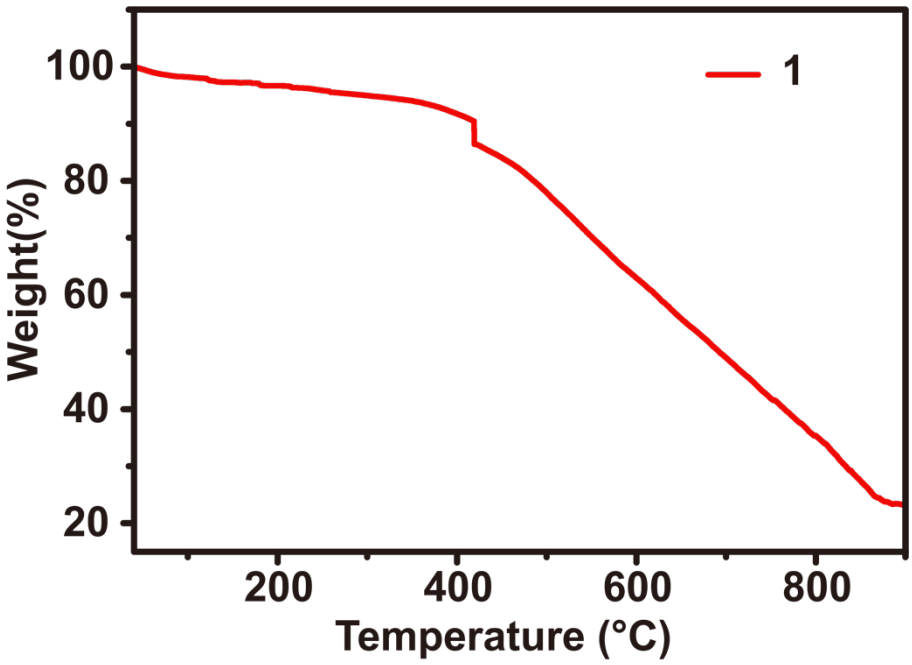

Figure S3. The thermogravimetric analysis (TGA) of the Y_{12} cluster

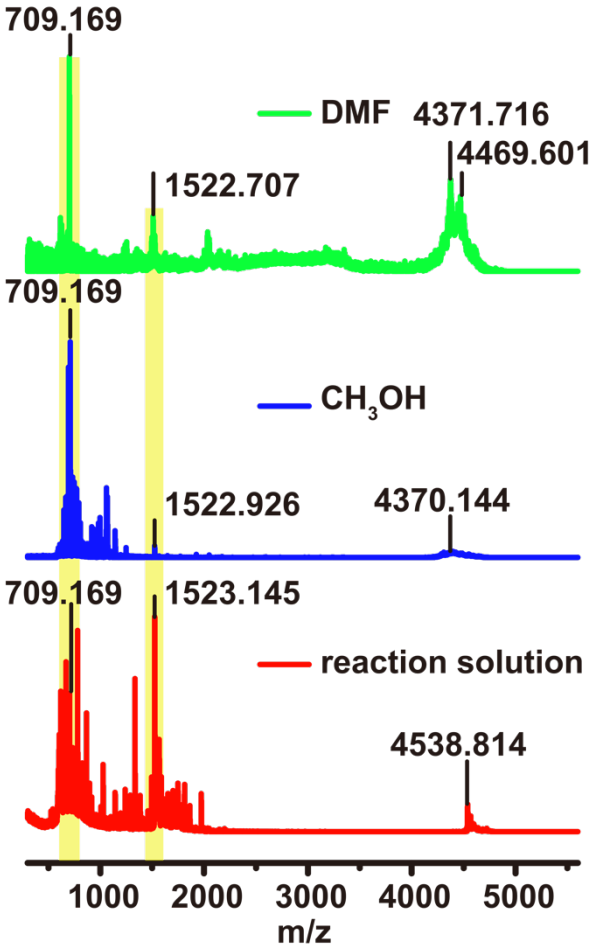

Figure S4. The ESI-MS spectra of **1** dissolved in DMF (green line) and MeOH (blue line) and the reaction solution.

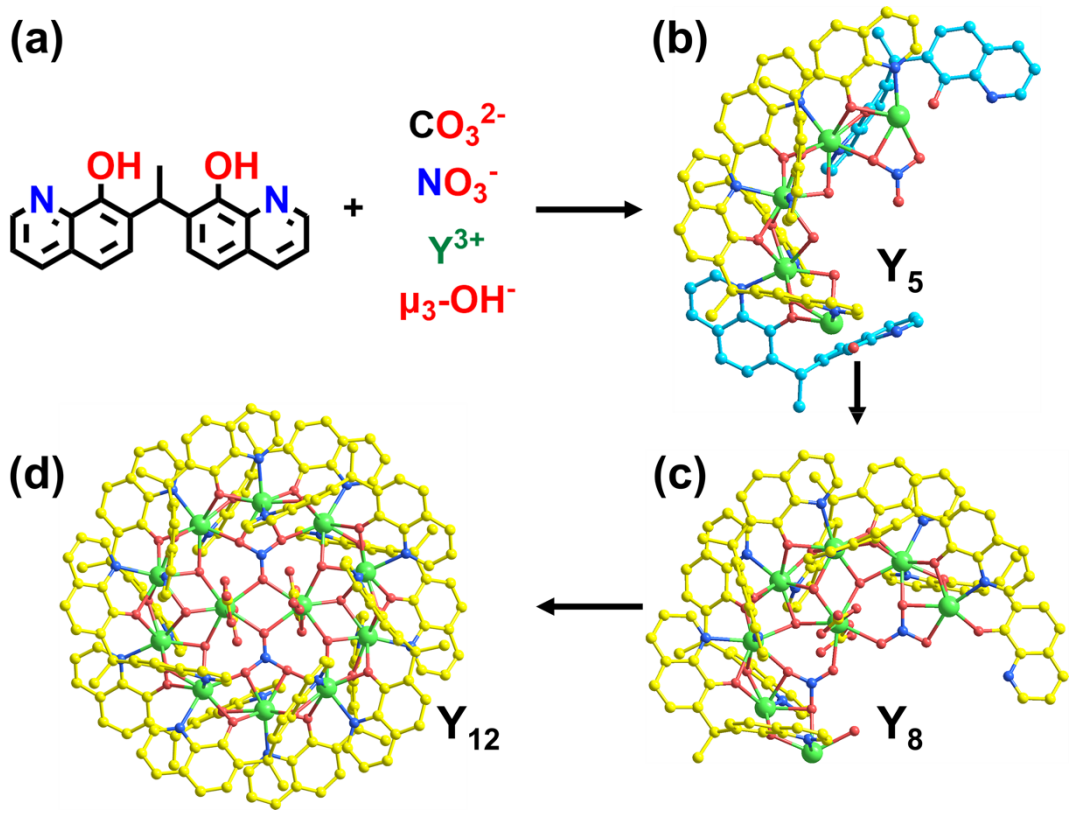

Figure S5. The possible self-assembly mechanism of Y_{12} cluster. (a) The *in-situ* ligand, Y^{3+} ions and other anions bridging ligands. (b) the structure diagram of Y_5 (the yellow ligands stand for L^{2-} and the cyan ligands stand for the HL^-). (c) and (d) the structure diagrams of Y_8 and Y_{12}, respectively.

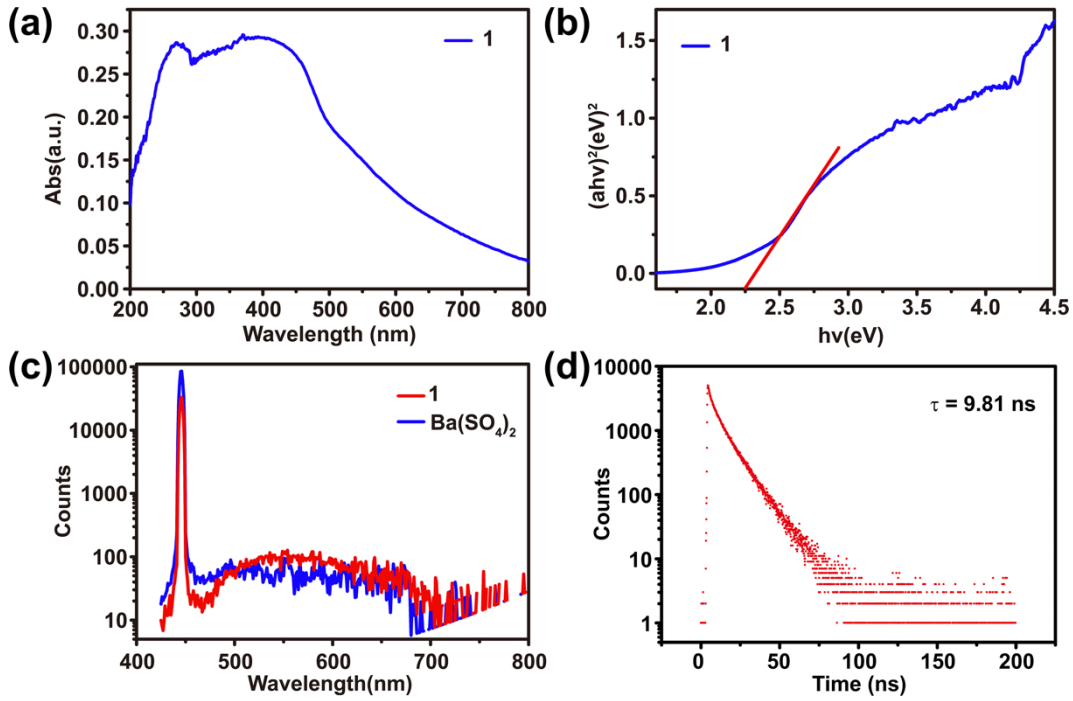

Figure S6. (a) The solid-state UV-vis spectrum of **1**. (b) The calculation result of the band gap of **1**. (c) The solid-state photoluminescence quantum yield of **1** at room temperature. (d) The photoluminescence decay profiles of **1** in bulk form at room temperature.

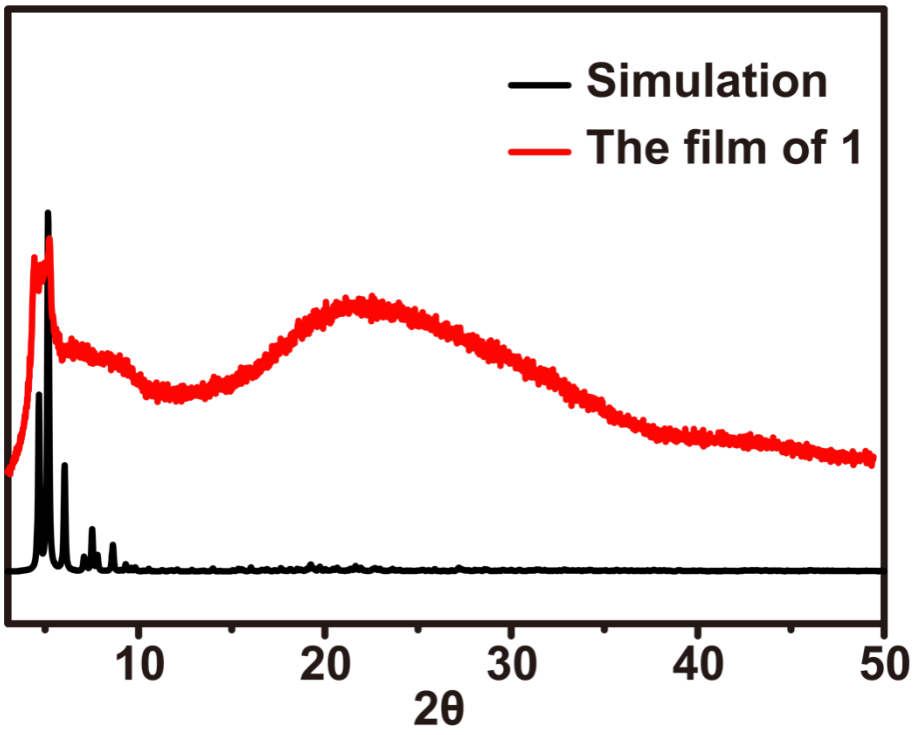

Figure S7. The PXRD pattern of the film of **1**.

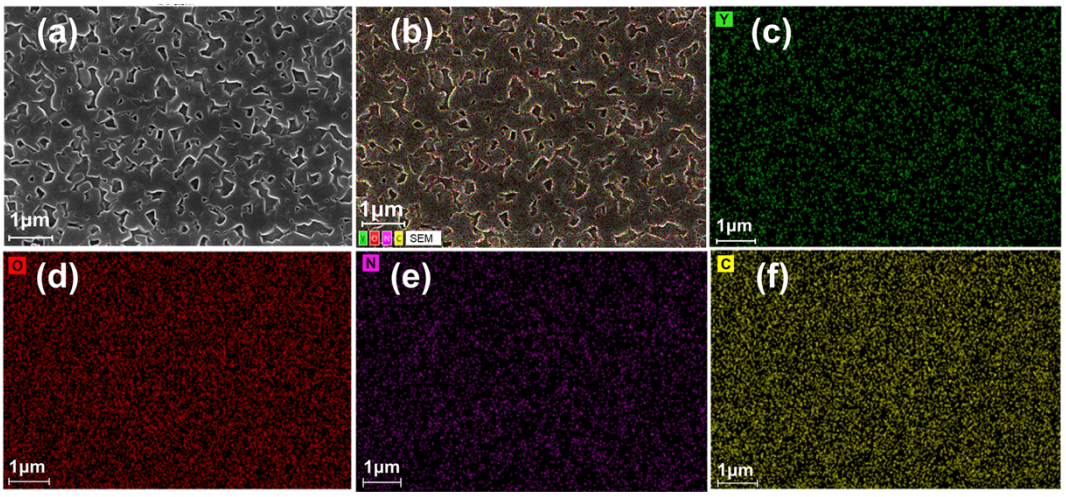

Figure S8. (a) The SEM images of the prepared thin film sample of the Y_{12} cluster on ITO. (b-f) the elemental mapping images of the thin film sample of the Y_{12} cluster on ITO.

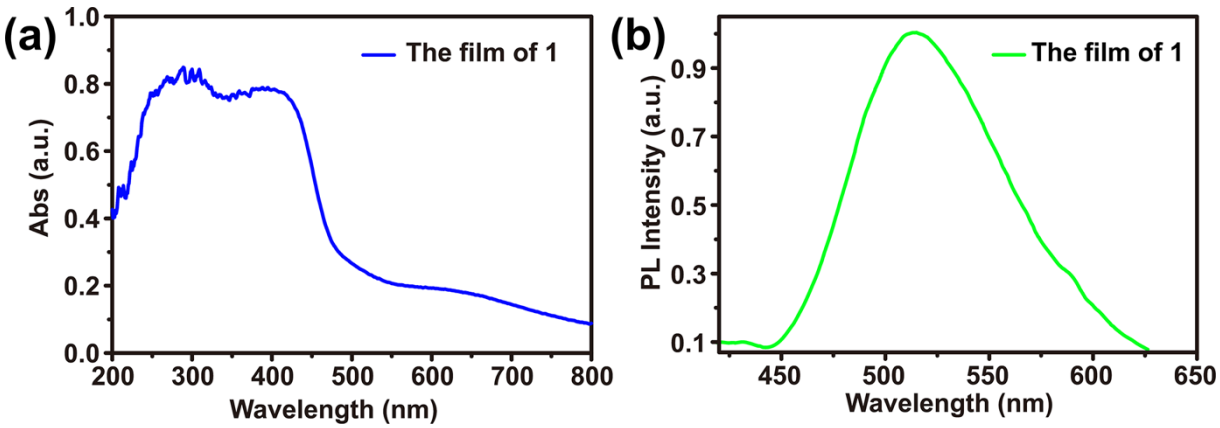

Figure S9. (a) The UV-vis spectrum of the film of **1**. (b) The emission spectrum of the film of **1**.

Table S1. The crystal data and structure refinement for **1** at 193 K.

Compound	**1**
Chemical Formula	$C_{204}H_{146}N_{22}O_{44}Y_{12}$
Formula weight	4676.34
Temperature (K)	193
Crystal system	triclinic
Space group	$P\bar{1}$
a, Å	17.5403(4)
b, Å	17.7051(4)
c, Å	19.9724(4)
α/°	74.5520(10)
β/°	78.8360(10)
γ/°	83.7730(10)
V, Å^3	5854.7(2)
Z	1
ρ calc g/cm^3	1.326
μ/mm^{-1}	4.359
F (000)	2344
Radiation	Cu Kα (λ = 1.54178)
Reflections collected	74952
Independent reflections	24594
Goodness-of-fit on F^2	1.079
Final R indexes [I>=2σ (I)]	R_1 = 0.0506, wR_2 = 0.1468
Final R indexes [all data]	R_1 = 0.0578, wR_2 = 0.1523

$R_1 = \Sigma||Fo|-|Fc||/\Sigma|Fo|$; $wR_2 = [\Sigma w(Fo^2-Fc^2)^2/\Sigma w(Fo^2)^2]^{1/2}$.

Table S2. Selected bond lengths [Å] for **1**.

Y1-O1^i	2.362(3)	Y4-O4	2.298(3)
Y1-O9	2.399(2)	Y4-O2	2.296(3)
Y1-O11	2.354(3)	Y4-O5	2.375(3)
Y1-O10	2.301(3)	Y4-O3	2.444(3)
Y1-O27	2.304(3)	Y4-O23	2.302(6)
Y1-O12	2.347(3)	Y4-O20	2.306(13)
Y1-N1^i	2.405(3)	Y4-N10	2.434(4)
Y1-N6	2.504(3)	Y4-N2	2.546(4)
Y1-N11	2.730(5)	Y4-O24	2.45(3)
Y2-O6	2.316(2)	Y4-O22	2.620(16)
Y2-O9	2.395(3)	Y4-O21	2.23(3)
Y2-O11	2.342(3)	Y4-O19	2.65(2)
Y2-O27	2.288(3)	Y5-O1	2.447(3)

Y2-O7	2.454(3)	Y5-O2	2.299(3)
Y2-O17	2.444(6)	Y5-O10^{i}	2.332(3)
Y2-N7	2.438(4)	Y5-O12^{i}	2.357(3)
Y2-N9	2.505(3)	Y5-O3	2.375(3)
Y2-O18	2.144(14)	Y5-O23	2.407(7)
Y2-N12	2.588(19)	Y5-N8^{i}	2.541(4)
Y2-O16	2.24(2)	Y5-N3	2.439(4)
Y3-O6	2.290(2)	Y5-N13	2.659(14)
Y3-O4	2.288(2)	Y5-O24	2.23(3)
Y3-O7	2.361(3)	Y5-O22	2.214(18)
Y3-O5	2.461(3)	Y6-O23	2.363(6)
Y3-O17	2.274(5)	Y6-O17	2.382(6)
Y3-O20	2.346(11)	Y6-O20	2.116(11)
Y3-N4	2.529(3)	Y6-O28	2.356(4)
Y3-N5	2.404(4)	Y6-O13^{i}	2.416(5)
Y3-O18	2.353(15)	Y6-O13	2.399(5)
Y3-O21	2.42(3)	Y6-O8	2.353(4)
Y3-O16	2.639(18)	Y6-O25	2.409(4)
Y3-O19	2.45(2)		

Symmetry codes: ^{i}1-x,1-y,1-z.

Table S3. Selected bond angles [°] for **1**.

Y1^{i}-O1-Y5	92.78(9)	Y3-O17-Y2	92.9(2)
Y4-O2-Y5	98.25(9)	Y3-O17-Y6	108.0(3)
Y5-O3-Y4	92.26(9)	Y6-O17-Y2	129.0(2)
Y3-O4-Y4	98.04(9)	Y2-O18-Y3	99.0(6)
Y4-O5-Y3	91.42(9)	Y3-O19-Y4	85.4(7)
Y3-O6-Y2	96.01(9)	Y4-O20-Y3	96.2(4)
Y3-O7-Y2	90.58(9)	Y6-O20-Y3	115.1(5)
Y2-O9-Y1	92.15(9)	Y6-O20-Y4	115.2(5)
Y1-O10-Y5^{i}	97.47(9)	Y4-O21-Y3	95.9(12)
Y2-O11-Y1	94.63(9)	Y4-O23-Y5	94.8(2)
Y1-O12-Y5^{i}	95.52(9)	Y4-O23-Y6	106.7(3)
Y6-O13-Y6^{i}	109.95(16)	Y6-O23-Y5	137.8(3)
Y2-O16-Y3	88.8(7)	Y2-O27-Y1	97.49(9)

Symmetry codes: ^{i}1-x,1-y,1-z.

Table S4. the bonds lengths and angles of the non-classical hydrogen bond (C-H···π interaction) in Y_{12} cluster.

C-H···π interaction	the distance between H and π-ring/(Å)	the angles of C-H···π/(°)
C49-H49···ring1	2.767	162
C34-H34···ring2	2.985	164

The ring1 is the benzene ring in quinoline group which constructed by C84, C85, C86, C87, C88 and C89 atoms. The ring 2 is the pyridine ring in quinoline group which constructed by N7, C95, C96, C, 98, C99 and C100 atoms.

Table S5. Identification of the key species in ESI-MS of complex **1**.

Species	Exp. m/z	Sim. m/z
$[Y_{12}(C_{20}N_2O_2H_{14})_9(CO_3)_4(NO_3)_2(\mu_3\text{-}OH)_7(H_2O)_5]^+$	4469.601	4469.080
$[Y_{12}[(C_{20}N_2O_2H_{14})_9(CO_3)_3(NO_3)_2(\mu_3\text{-}OH)_9(H_2O)]^+$	4371.716	4371.025
$[Y_{12}(C_{20}N_2O_2H_{14})_9(CO_3)_4(NO_3)(\mu_3\text{-}OH)_8(H_2O)_2]^+$	4370.144	4370.037
$[Y_8(C_{20}N_2O_2H_{14})_6(CO_3)_2(NO_3)_2(\mu_3\text{-}OH)_4(CH_3CH_2OH)_3]^{2+}$	1523.145	1523.765
$[Y_5(C_{20}N_2O_2H_{14})_3(C_{20}N_2O_2H_{15})_2(NO_3)(\mu_3\text{-}OH)_3]^{3+}$	709.169	709.83

Tbale S6. Summary of the electroluminescence performance of the OLED devices based on some rare-earth/transition metal clusters or mono-nuclear complexes.

Cluster	Quantum Yield (%)	Turn-on voltage (V)	Max luminance (cd/m^2)	Ref.
Y_{12} cluster	4.95	4	84	this work
$[Tb\{Tb_4(hpmba)_8(\mu_3\text{-}OH)_4(\mu_4\text{-}OH)\}_2OH]$	--	7	--	7
$[Eu(tapo)_2(tta)_3]$	39.4	4.4	1195	8
$Tb(PA^2)_3(H_2O)_2$	33	8	20	9
$[Ce(triPrNTB)_2](SO_3CF_3)_3{\cdot}2H_2O$	55	9.1	1.5	10
$Tb(eb\text{-}PMP)_3TPPO$	--	11	46	11
$Dy(PM)_3(TP)_2$	3.5	11.9	524	12
$[Au_4(P\hat{}P\hat{}P)_2(C_2R)_2]^{2+}$ R: $C_6H_4NMe_2$	51	2.5	7430	13
R/S-NHC^{ql}-Au-Cu cluster	20.8	6.5	5600	14

References:

[1] M.-M. Wu, J.-Y. Wang, R. Sun, C. Zhao, J.-P. Zhao, G.-B. Che and F.-C. Liu, *Inorg. Chem.*, 2017, **56**, 9555-9562.

[2] X.-W. Liang, L.-L. Zhang, T. Zhang, J.-P. Zhao and F.-C. Liu, *Dalton Trans.*, 2022, **51**, 8491–8496.

[3] O. V. Dolomanov, L. J. Bourhis, R. J. Gildea, J. A. K. Howard, and H. Puschmann, *J. Appl. Cryst.*, 2009, **42**, 339–341.

[4] G. M. Sheldrick, *Acta Crystallogr. Sect. C: Struct. Chem.*, 2015, **71**, 3-8.

[5] Y. Kashiwagi, K. Kubono and T. Tamai, *Acta Cryst. E.*, 2020, **76**, 1271-1274.

[6] X.-M. Zhang, J.-Q. Li, S.-J. Liu, M.-B. Luo, W.-Y. Xu and F. Luo, *CrystEngComm*, 2014, **16**, 2570-2573.

[7] H.-B. Xu, X.-F. Li and D. Yan, *Inorg. Chem. Commun.*, 2008, **11**, 1187-1189.

[8] H. Xu, K. Yin and W. Huang, *Chem. Eur. J.*, 2007, **13**, 10281-10293.

[9] V. V. Utochnikova, E. V. Latipov, A. I. Dalinger, Y. V. Nelyubina, A. A. Vashchenko, M. Hoffmann, A. S. Kalyakina, S. Z. Vatsadze, U. Schepers, S. Bräse and N. P. Kuzmina, *J. Lumin.*, 2018, **202**, 38-46.

[10] X.-L. Zheng, Y. Liu, M. Pan, X.-Q. Lü, J.-Y. Zhang, C.-Y. Zhao, Y.-X. Tong and C.-Y. Su, *Angew. Chem. Int. Ed.*, 2007, **46**, 7399–7403.

[11] H. Xin, F. Y. Li, M. Shi, Z. Q. Bian and C. H. Huang, *J. Am. Chem. Soc.*, 2003, **125**, 7166-7167.

[12] Z.-F. Li, L. Zhou, J.-B. Yu, H.-J. Zhang, R.-P. Deng, Z.-P. Peng and Z.-Y. Guo, *J. Phys. Chem. C*, 2007, **111**, 2295-2300.

[13] T. M. Dau, Y.-A. Chen, A. J. Karttunen, E. V. Grachova, S. P. Tunik, K.-T. Lin, W.-Y. Hung, P.-T. Chou, T. A. Pakkanen and I. O. Koshevoy, *Inorg. Chem.*, 2014, **53**, 12720-12731.

[14] X.-H. Ma, J. Li, P. Luo, J.-H. Hu, Z. Han, X.-Y. Dong, G. Xie and S.-Q. Zang, *Nat. Commun.*, 2023, **14**, 4121.